The extravascular implantable cardioverter-defibrillator: characterization of anatomical parameters impacting substernal implantation and defibrillation efficacy

Levente Molnár[1], Ian Crozier[2], Haris Haqqani[3], David O'Donnell[4], Emily Kotschet[5], Jeffrey Alison[5], Amy E. Thompson[6], Varun A. Bhatia[6], Roland Papp[1], Endre Zima[1], Ádám Jermendy[1], Astrid Apor[1], and Béla Merkely ⓘD [1]*

[1]Semmelweis University, Heart and Vascular Center, 68, Varosmajor Street, H-1122 Budapest, Hungary; [2]Department of Cardiology, Christchurch Hospital, PO Box 4345, Christchurch, New Zealand; [3]Faculty of Medicine, University of Queensland, Department of Cardiology, Prince Charles Hospital, Brisbane, Australia; [4]Department of Cardiology, Austin Health, Heidelberg, Victoria, Australia; [5]Monash Cardiac Rhythm Management Department, MonashHeart, Monash Medical Centre, 246 Clayton Road, Clayton, Melbourne, Victoria, 3168, Australia; and [6]Medtronic plc, Mounds View, Minneapolis, MN, USA

Aims	The aim of this study is to provide a thorough, quantified assessment of the substernal space as the site of extra-vascular implantable cardioverter-defibrillator (ICD) lead placement using computed tomography (CT) scans and summarizing adverse events and defibrillation efficacy across anatomical findings. Subcutaneous ICDs are an alternative to transvenous defibrillators but have limitations related to ICD lead distance from the heart. An alternative extravascular system with substernal lead placement has the potential to provide defibrillation at lower energy and pacing therapies from a single device.
Methods and results	A multi-centre, non-randomized, retrospective analysis of 45 patient CT scans quantitatively and qualitatively assessing bony, cardiac, vascular, and other organ structures from two human clinical studies with substernal lead placement. Univariate logistic regression was used to evaluate 15 anatomical parameters for impact on defibrillation outcome and adjusted for multiple comparisons. Adverse events were summarized. Substernal implantation was attempted or completed in 45 patients. Defibrillation testing was successful in 37 of 41 subjects (90%) using ≥10 J safety margin. There were two intra-procedural adverse events in one patient, including reaction to anaesthesia and an episode of transient atrial fibrillation during ventricular fibrillation induction. Anatomical factors associated with defibrillation failure included large rib cage width, myocardium extending very posteriorly, and a low heart position in the chest (P-values <0.05), though not significant adjusting for multiple comparisons.
Conclusion	Retrospective analysis demonstrates the ability to implant within the substernal space with low intra-procedural adverse events and high defibrillation efficacy despite a wide range of anatomical variability.
Keywords	Implantable cardioverter-defibrillator • Extravascular • Substernal • Anterior mediastinum • Tachyarrhythmia

What's new?

- The substernal space represents a compelling option for extravascular lead placement, potentially overcoming limitations of transvenous and subcutaneous implantable cardioverter-defibrillators (ICDs).
- An extravascular ICD (EV ICD) system with novel lead placement in the substernal space may provide an implantable defibrillator option for patients at risk of sudden cardiac death who could benefit from extravascular system placement and pacing therapies such as antitachycardia pacing in a single implantable device.
- Because the substernal space offers a unique relationship between the defibrillation coil and surrounding anatomy, an understanding of anatomical and implantation factors will be required to maximize safety and efficacy with substernal lead placement and defibrillation.
- Presented here is the first comprehensive computed tomography-based analysis of subjects with substernal lead placement describing a range of structure measurements and the corresponding defibrillation efficacy and adverse events across varying patient anatomies.

Introduction

For decades, transvenous implantable cardioverter-defibrillators (TV ICDs) have represented the device-based standard of care for patients with arrhythmia risk, yet issues such as vascular injury, lead fracture, and vessel occlusions have persisted as impediments to TV ICD usage, creating demand for extravascular systems.[1] While the subcutaneous ICD (SQ ICD) has emerged as an alternative to TV ICD, the distance of the SQ lead from the heart has resulted in an SQ ICD that does not offer antitachycardia pacing (ATP) and requires greater energy for defibrillation, using a larger device with potential patient comfort issues and reduced longevity.[1,2]

The substernal space (anterior mediastinum) is an intriguing area for lead implantation due to proximity to the heart. Acute human studies have demonstrated the feasibility of implanting within the substernal space and delivering pacing and defibrillation therapies.[3–5] More recently, the first-in-human chronic experience of the extravascular ICD (EV ICD) with substernal lead placement was reported, demonstrating a 90-day freedom from system/procedure major complication rate of 94.1% and a defibrillation efficacy of 90% when testing for a ≥ 10 J safety margin.[6]

The substernal space is often accessed for cardiac and non-cardiac medical procedures, including sternotomy for cardiac surgery, lung metastasectomy and tumour excision, thymectomy, pectus excavatum revisions, and mediastinoscopy.[7–11] While comparative procedures to access the mediastinal space exist, the EV ICD implant procedure is unique and has anatomical considerations unlike other procedures, requiring an understanding of the natural variation of substernal anatomy for procedural and therapeutic success.

Anatomists have quantified limited aspects of the substernal space previously.[12,13] However, a thorough, quantified assessment, including neighbouring cardiac, vascular, pleural, and musculoskeletal regions, has not been offered. We present a computed tomography (CT)-based analysis of subjects with substernal lead placement to describe a range of structure measurements and the corresponding defibrillation efficacy and adverse events across varying patient anatomies.

Methods

Study design

This is a multi-centre, non-randomized, retrospective analysis from two human clinical evaluations: The Acute Extravascular Defibrillation, Pacing, and Electrogram Study (ASD2) and the first-in-human chronic evaluation of the EV ICD system (pilot study), whose methodologies have been reported previously.[5,6] Both studies complied with the Declaration of Helsinki[14] and were approved by the ethics committee(s) and associated regulatory authorities. Informed consent was obtained from all patients before enrolment.

Data from 45 subjects from the ASD2 and pilot studies that underwent an EV ICD implantation attempt and had a CT scan on file were analysed, representing participation from five sites in Hungary, Australia, and New Zealand.

Study population

In the ASD2 study, eligible patients were those undergoing a surgical procedure requiring midline sternotomy or implant of a TV ICD or SQ ICD.[5] In the pilot study, eligible patients were those undergoing ICD implantation with a Class I or IIa indication based on current clinical guidelines.[6,15]

Implant procedure

In the ASD2 study, pre-procedural fluoroscopy was required in both lateral and anteroposterior (AP) views prior to substernal tunnelling, and CT scans could be collected per physician discretion. For the chronic pilot study, pre-procedural CT images were required. In both studies, if the investigator determined that a subject's anatomy could not accommodate the implant tools (e.g. the tunnelling tool could not maintain close proximity to the sternum during tunnelling), then the procedure was not continued.

The EV ICD lead is implanted via a minimally invasive subxiphoid approach.[6] After marking the xiphoid process, rib margin, sternal midline, left lateral sternal border, and the top of the cardiac silhouette, a small incision is made proximate and leftward the xiphoid process. Blunt dissection is used to facilitate entry through the diaphragmatic attachments and into the anterior mediastinum. Confirmation of substernal entry is performed by inserting a finger into the tunnelling tract and feeling the underside of the sternum prior to introduction of the tunnelling tool. A blunt tunnelling rod backloaded with a 9-Fr introducer sheath is then introduced into the substernal space and using alternating lateral and AP fluoroscopic views is tunnelled approximately at or just left of the sternal midline. The tunnelling tool is then removed and the sheath retained within the substernal space, through which the lead is introduced. After acute electrical testing, the sheath is removed, and the lead secured at an anchoring sleeve near the incision site.

In the chronic pilot study, the ICD was positioned in a subcutaneous device pocket on the left chest near the left midaxillary line at physician discretion. Because ASD2 was an acute study, a cutaneous patch electrode (Covidien Model 1010P multi-function defibrillation electrode) was used predominantly, mimicking an ICD without adding additional incisions. The cutaneous electrode was adhered on the subject's skin,

centred on the left midaxillary line at approximately the 5th intercostal space.

Extravascular implantable cardioverter-defibrillator system design

The EV ICD lead is an 8.7-Fr epsilon-shaped passive fixation lead with two pace-sense rings and two defibrillation coils. The EV ICD system can deliver up to 40 J for defibrillation and provide ATP, post-shock pacing, and asystole support pacing.[6]

Computed tomography analysis procedures

Volumetric CT scans were obtained with an in-plane resolution and slice thickness of ~1.0 mm or better prior to implant. The CT images were segmented by tissue type using Materialise Mimics 21.0 software (Leuven, Belgium). Descriptive and quantitative measurements were taken, with the specific anatomical measurements and their methods summarized in *Table 1*.

Adverse event characterization

Procedure- and system-related intra-procedural adverse events were assessed for all subjects and adjudicated by an independent committee.

Defibrillation efficacy characterization

For all subjects, defibrillation efficacy at implant was assessed using a ≥ 10 J safety margin for a 40 J device. In the ASD2 study, up to two episodes of ventricular tachycardia/ventricular fibrillation (VT/VF) were induced per subject, and a single 30 J shock was delivered after each induction. In the pilot study, a defibrillation testing protocol was used that first evaluated success of a single 20 J shock, and if not successful, evaluated the success of a 30 J shock on two consecutive episodes of VF. To create a common definition of success across both clinical protocols, defibrillation success hereafter will be defined as success on first induction at maximum tested energy (20 or 30 J) in the final lead and device position, regardless of polarity.

Statistical analyses

The SAS 9.4 was utilized for all analyses. Descriptive statistics were used to summarize baseline demographics and shock impedance by study. Univariate logistic regression tests were performed to assess whether any of 15 variables affected defibrillation success. Study was not accounted for in these analyses. Odds ratios and 95% confidence intervals were generated for each variable, and the *P*-values were adjusted for multiple comparisons using the Holm procedure.

Results

A total of 45 subjects underwent the substernal implantation procedure (*Figure 1*). The CT scans of 45 subjects were analysed from the ASD2 (*n* = 24) and pilot (*n* = 21) studies, representing subjects from Hungary (*n* = 16), Australia (*n* = 13), and New Zealand (*n* = 16). The cohort was 84% male and the average age was 58 ± 13 (mean ± standard deviation) years, though age differed by study (ASD2: 62 ± 10, pilot: 54 ± 14). Subjects had a left ventricular ejection fraction (LVEF) of 38.2 ± 15.7% (range: 20–80%) and an average body mass index (BMI) of 30.0 ± 4.4 (*Table 2*).

Anatomical characterization

Characterization of bony and cartilaginous structures included measurements of the xiphoid process, sternum, and rib cage. The xiphoid process across subjects varied in shape but was readily divided into one of three main classifications: straight (40%), curved (29%), or bifurcated (31%), while the most common sternal shape was a longitudinal oval (64%). The length of the xiphoid process was variable, ranging from 22 to 69 mm, while the sternal body length ranged from 76 to 129 mm and was 27–61 mm wide at its widest point (40 ± 8 mm). The average chest circumference ranged from 71 to 128 cm, while the mean width of the rib cage in the left-to-right direction ranged from 240 to 320 mm and rib cage thickness in the AP direction ranged from 167 to 273 mm.

Various cardiac-related and vascular structures were characterized. The volume of the heart varied substantially, ranging from 683 to 2052 cm^3 (*Figure 2*, left image). The separation between the heart and sternum was also evaluated (*Figure 2*, right image). At its nearest point, the heart was 6.5 ± 4.0 mm from the sternum (range: 0–16 mm), while at its maximum distance, the heart was 14.8 ± 6.8 mm from the sternum (range: 4–35 mm). At the xiphisternal junction near the lead insertion site, the heart distance from the sternum measured 8.1 ± 4.5 mm (range: 2–19 mm).

The orientation and reach of the heart varied, with the leftmost extent of the myocardium extending 72–122 mm from the mid-sternum, and the posterior extent of the myocardium extending 79–149 mm from the sternum (*Figure 3*, left and middle images). Measuring from the xiphisternal junction, the most superior aspect of the heart extended 10–100 mm upwards and the inferior-most heart extended 20–100 mm downwards (*Figure 3*, right image). The ratio of inferior-to-superior reach of the heart measured 1.3 ± 1.4 (range: 0.2–8.5).

The internal thoracic vessels were offset from the lateral edges of the sternum in all subjects and the superior epigastric artery was offset from the xiphoid process (*Figure 4*, left image). Measuring from the level of the xiphisternal junction, the left internal thoracic artery (ITA) was offset from the sternum by a range of 12–37 mm, while along the length of the sternal body, the shortest distance from the sternum to the ITA ranged from 6 to 23 mm.

The right or left lung crossed behind the sternum in most subjects (43 and 41 subjects, respectively) and touched in 17 of 45 subjects (37.8%). Qualitative assessment of the rib level at which the lungs crossed behind the sternum (*Figure 4*, right image) revealed that the right lung most frequently crossed behind the sternum at the level of the fifth or sixth rib (in 9 and 12 subjects, respectively) or at the level of the xiphisternal junction (in 11 subjects). The left lung most frequently crossed at the level of the third or fourth rib (in 12 and 16 subjects, respectively), and never crossed beneath the sternum at the level of the xiphisternal junction or inferior to it.

On average, the liver was 40.6 ± 16.2 mm inferior to the xiphisternal junction (range: 10–81 mm). Anatomical measures are summarized in *Table 3*.

Defibrillation efficacy

Defibrillation testing at implantation was completed in 41 subjects, and defibrillation was successful in 37 subjects (90%) using a ≥ 10 J safety margin for testing. Among four subjects with shock failure, two

Table I Anatomical measurement methodologies

Anatomical measurement	Measurement method
Bony and cartilaginous measures	
1. Xiphoid size and shape	• Size: length of xiphoid process from the xiphisternal junction to the inferior-most tip of the xiphoid process (mm) • Shape: qualitative assessment of xiphoid shape
2. Sternum size and shape	• Size: length of the sternum from the manubrial-sternal junction to the xiphisternal junction (mm) and maximum width of the sternum • Shape: qualitative assessment of sternal shape
3. Chest dimensions	• Average chest circumference from in-office tape measurement (mm) • AP measurement of rib cage, measuring from posterior surface of sternum to spinous process (mm), in the axial slice, at the level of the xiphisternal junction • Left–right rib cage, measuring the widest dimension of the rib cage from left lateral edge to right lateral edge (mm)
Cardiac and vascular measures	
4. Heart volume	• Volume of the segmented epicardium (including blood pool, cm^3)
5. LV myocardium thickness	• Thickness at tip of posterior papillary muscle, short-axis view
6. LV mass	• LV myocardial volume times 1.055
7. Extent of heart	• Maximum distance from mid-sternum to left-most and right-most extent of the myocardium (mm) • Overall left-to-right distance: Overall distance from right-most to the left-most border of the myocardium (mm)
8. Posterior-most extent of heart	• Maximum distance from posterior surface of sternum to posterior-most extent of the myocardium (mm)
9. Superior and inferior heart distances	• Bottom- and top-most extent of heart (in superior direction, top of atrial myocardium), relative to xiphisternal junction (mm) • Overall superior-to-inferior boundary distance: The distance from the superior boundary to the inferior boundary of the heart (mm) • Inferior-to-superior ratio: Inferior distance of myocardium from the xiphisternal junction divided by the superior distance of myocardium from the xiphisternal junction
10. Sternum-to-heart distance	• Axial views: distance from posterior surface of sternum to peri/epicardium, every 10 mm starting proximate the xiphisternal junction and moving superiorly, at the left sternal edge (mm)
11. Internal thoracic artery	• Axial views: the minimum distance from lateral border of sternum to internal thoracic artery, starting at the xiphisternal junction or xiphoid tip to the level of the manubrial-sternal junction (mm) • The distance from xiphisternal junction to left internal thoracic artery directly lateral to the xiphisternal junction (mm)
Lung measures	
12. Lung intercedence	• Qualitative assessment of whether the left and right lung cross behind the sternum, including at which rib level, using the axial view within the boundaries of the top/bottom of heart; qualitative assessment of whether the lungs touch one another
Liver measures	
13. Liver location	• Axial view: relative to left and right sternal borders, the distance from xiphisternal junction to liver at each border (mm)
Fat thickness measures	
14. Fat distribution	• Epicardial fat thickness: the measured distance between epicardium and pericardium at multiple axial slices, at the xiphisternal junction and along the right ventricle behind the sternum (mm) • Apical fat thickness: the measured distance between epicardium and pericardium, at the apex in the short-axis view (mm)

A listing of the measurements taken and their methodologies.
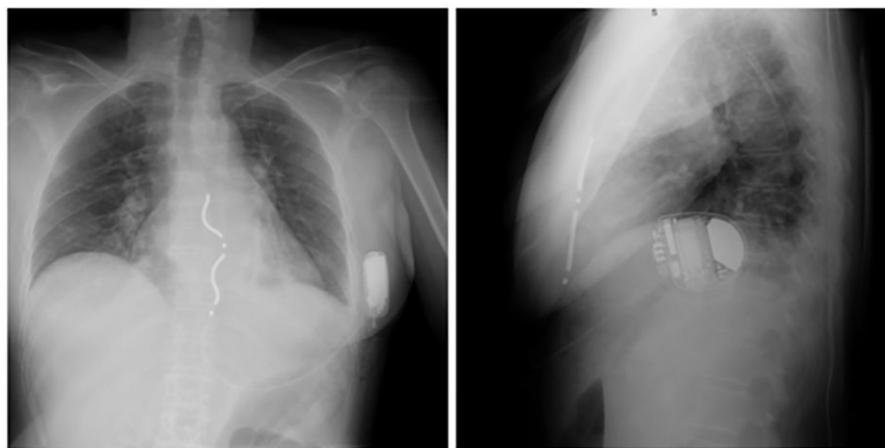AP, anteroposterior; LV, left ventricular.

Figure 1 Implanted EV ICD system. Representative image of the EV ICD system *in situ* as shown in anteroposterior (left) and lateral (right) fluoroscopy. ICD, extravascular implantable cardioverter-defibrillator.

Table 2 Baseline characteristics

Patient characteristics	ASD2 (N = 24)	EV ICD pilot (N = 21)	P-value[a]	Total cohort (N = 45)
Male	21 (87.5%)	17 (81.0%)	0.689	38 (84.4%)
Age (years)			**0.031**	
Mean ± standard deviation	62.1 ± 10.1	54.2 ± 13.8		58.4 ± 12.5
Range	34.0–77.0	21.5–77.4		21.5–77.4
LVEF (%)			0.079	
Mean ± standard deviation	34.3 ± 12.2	42.6 ± 18.2		38.2 ± 15.7
Range	20–76	20–80		20–80
Height (cm)			0.136	
Mean ± standard deviation	177.5 ± 9.6	173.3 ± 8.9		175.5 ± 9.5
Range	159–200	150–186		150–200
BMI (kg/m^2)			0.202	
Mean ± standard deviation	29.2 ± 4.2	30.9 ± 4.6		30.0 ± 4.4
Range	20.6–35.7	22.4–37.6		20.6–37.6
NYHA functional class			0.679	
No HF	2 (8.3%)	4 (19.0%)		6 (13.3%)
I	9 (37.5%)	8 (38.1%)		17 (37.8%)
II	10 (41.7%)	8 (38.1%)		18 (40.0%)
III	3 (12.5%)	1 (4.8%)		4 (8.9%)
Cardiac arrest	3 (12.5%)	4 (19.0%)	0.689	7 (15.6%)
Cardiomyopathy, ischaemic	12 (50.0%)	7 (33.3%)	0.366	19 (42.2%)
Cardiomyopathy, non-ischaemic	6 (25.0%)	4 (19.0%)	0.729	10 (22.2%)
Cardiomyopathy, hypertrophic	0 (0%)	6 (28.6%)	**0.007**	6 (13.3%)
Coronary artery disease	6 (25.0%)	11 (52.4%)	0.073	17 (37.8%)
Hypertension	15 (62.5%)	11 (52.4%)	0.555	26 (57.8%)
Myocardial infarction	7 (29.2%)	7 (33.3%)	1.000	14 (31.1%)

Characteristics are reported for all subjects (*n* = 45).
ASD2, The Acute Extravascular Defibrillation, Pacing and Electrogram Study; BMI, body mass index; EV ICD, extravascular implantable cardioverter-defibrillator; LVEF, left ventricular ejection fraction.
[a]Two-sample *t*-tests were used to compare age, LVEF, height, and BMI between studies, while Fisher's exact test was used to compare the qualitative variables.
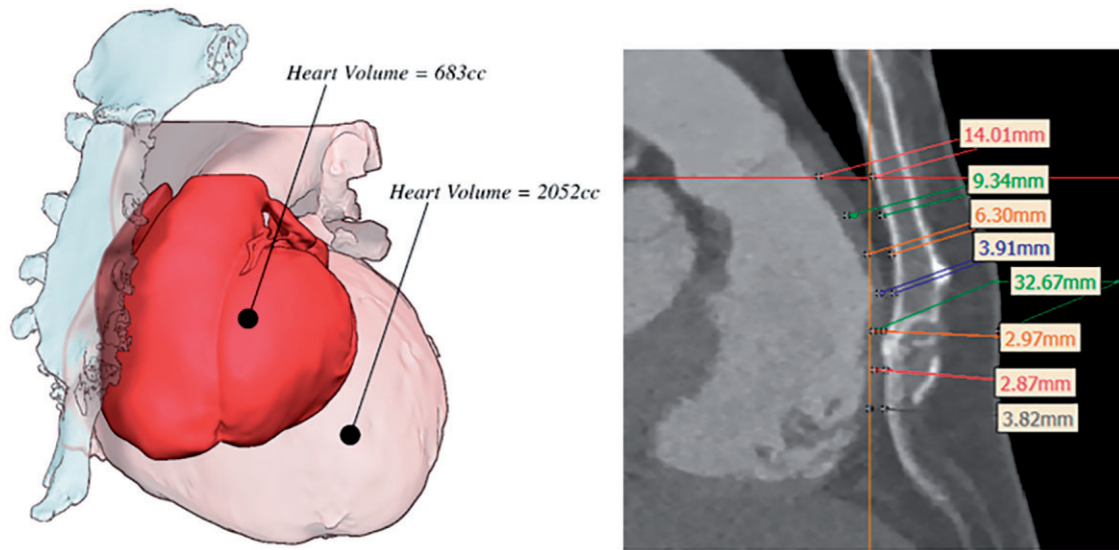
Figure 2 Heart volume and sternum-to-heart distance. The minimum and maximum heart volumes (left image) and a representative example of the distance from the sternum to the heart (right image).
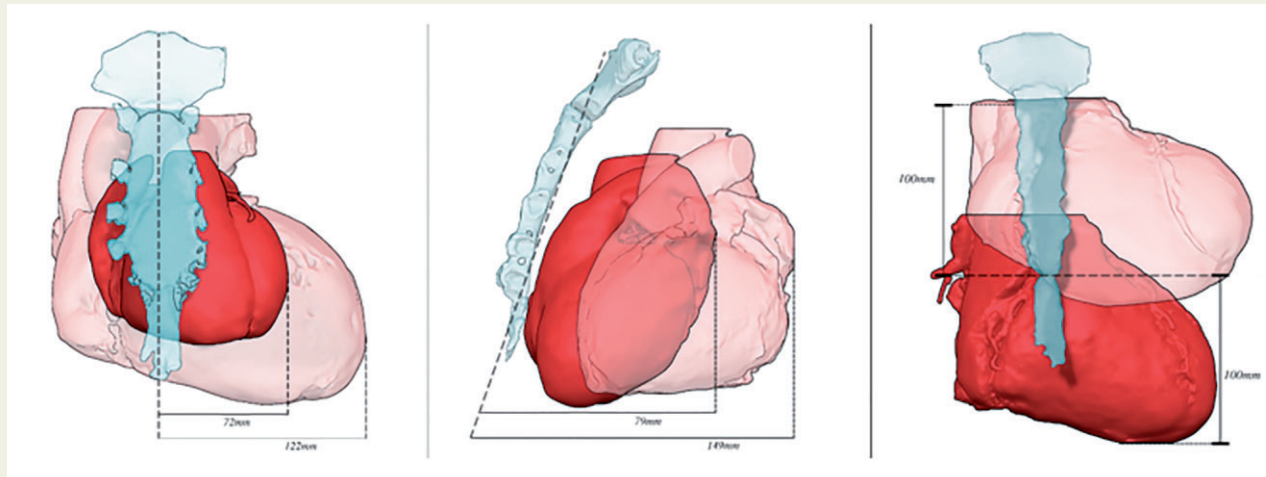

Figure 3 Myocardial extent in the leftward, posterior, and superior/inferior directions. Leftward extent (left image) shows the minimum and maximum distances from mid-sternum to the leftmost myocardium; posterior extent (middle image) shows the minimum and maximum distances from posterior sternum to posterior myocardium; and the superior and inferior extent (right image) are shown as the maximum distances from the xiphisternal junction to the most superior and inferior heart borders.

were from the ASD2 study and two were from the pilot study. Average shock impedance was significantly different between subjects from the chronic pilot study with full system implantation vs. the ASD2 acute study where a cutaneous patch electrode was used predominantly ($P < 0.0001$). Among subjects with 30 J first shock success, average impedance was 91.7 ± 22.0 Ω in the ASD2 study ($n = 19$ subjects) and 66.7 ± 10.3 Ω in the pilot study ($n = 18$ subjects). Among subjects with 30 J first shock failure, average impedance was 107.5 ± 31.8 Ω in the ASD2 study ($n = 2$ subjects) and 78.0 ± 1.4 in the pilot study ($n = 2$ subjects). In both studies, the observed average

impedance was lower in subjects with defibrillation success compared with failure.

Univariate logistic regression tests were performed to assess whether any of 15 anatomical variables affected shock success (*Table 4*). Anatomical factors associated with defibrillation failure included larger rib cage width in the left–right direction, a very posterior cardiac reach, and low heart position in the thorax. However, if adjusting for multiple analyses using the Holm procedure, the tests would not be significant, as the smallest *P*-value (0.028) would exceed the adjusted alpha level 0.05/15 = 0.0033.
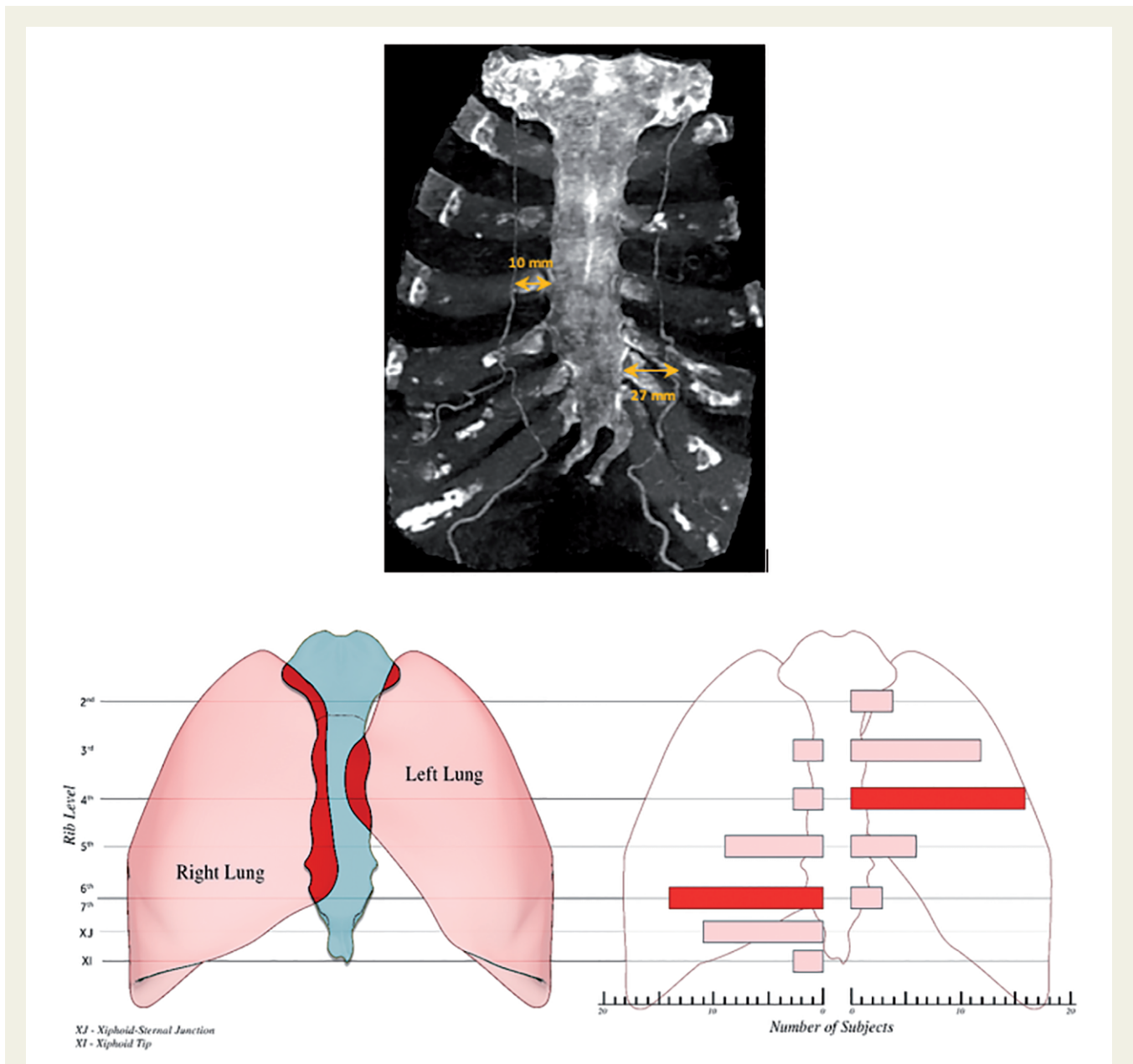
Figure 4 Internal thoracic artery, superior epigastric artery, and lung intercedence. A representative image of the left ITA offset from the xiphisternal junction and left sternal border, also showing the left anterior oblique view (~10°) of the superior epigastric artery offset from the xiphoid process (top image); the locations and frequency of lung crossing substernally (bottom images).

The parameter with the smallest *P*-value (0.028) was the posterior reach of the heart. For exemplary purposes, a graphical representation of the univariate statistical analysis for this parameter is provided, showing an estimate of shock success as a function of increasing reach of the myocardium in the posterior direction (*Figure 5*). As shown, each of the four defibrillation failures observed was associated with myocardium that extended >128 mm in the posterior direction; however, 8 of 37 subjects with shock success also had a posterior reach this great. At a posterior reach of 139 mm, the estimated defibrillation efficacy was 66% and the upper 95% confidence bound for estimated defibrillation efficacy fell below 90%.

Similarly, all four subjects with defibrillation failure had a left–right rib cage width >270 mm, though 20 subjects with defibrillation success had a rib cage at least this wide. The first and fourth widest rib cages were both defibrillation failures.

Hearts set low in the chest were associated with defibrillation failure, both when reflected as increased distance of the heart in the inferior direction and decreased distance in the superior direction. The first and second greatest distances from the xiphisternal junction to the inferior heart border were both defibrillation failures. In one subject, the heart extended 85 mm inferiorly with only 10 mm of heart extending superiorly while the other extended 100 mm inferiorly with only 26 mm extending superiorly. Similarly, for subjects with

Table 3 Summary of anatomical measurements [a]

Measurement	Mean ± SD (range)		
Bony and cartilaginous measures			
Xiphoid length	45.8 ± 11.8 (22–69) mm		
Xiphoid shape	Straight = 18 (40%), bifurcated = 14 (31%), curved = 13 (29%)		
Sternum size (Maximum width)	39.9 ± 7.5 (27–61) mm		
Sternum shape	Cup = 4 (9%), longitudinal oval = 29 (64%), flat = 12 (27%)		
Chest circumference	105.8 ± 12.6 (71–128) cm		
AP rib cage dimension	224.1 ± 23.7 (167–273) mm		
Left–right rib cage width	272.7 ± 18.3 (240–320) mm		
Cardiac and vascular measures			
Heart volume	1158.6 ± 304.8 (683–2052) cm^3		
LV myocardium thickness	10.9 ± 3.0 (6.5–20) mm		
LV mass	246.5 ± 83.8 (124–487) g		
Minimum sternum-to-heart distance	6.5 ± 4.0 (0–16) mm		
Maximum sternum-to-heart distance	14.8 ± 6.8 (4–35) mm		
Average sternum-to-heart distance	10.3 ± 4.9 (2.5–22.5) mm		
Sternum-to-heart distance at xiphisternal junction	8.1 ± 4.5 (2–19) mm		
Left internal thoracic artery	13.5 ± 4.1 (6–23) mm		
(Minimum distance from left sternal border)			
Left internal thoracic artery	24.6 ± 6.8 (12–37) mm		
(Distance from left sternal border at xiphisternal junction)			
Boundaries of the heart			
Inferior extent	52.1 ± 19.4 (20–100) mm		
Superior extent	53.8 ± 19.8 (10–100) mm		
Overall superior-to-inferior boundary distance	105.9 ± 15.0 (75–144) mm		
Left extent	99.6 ± 10.7 (72–122) mm		
Right extent	50.8 ± 9.1 (33–72) mm		
Overall left-to-right distance	150.4 ± 15.4 (118–187) mm		
Posterior extent	119.7 ± 14.7 (79–149) mm		
Inferior-to-superior ratio	1.3 ± 1.4 (0.2–8.5)		
Lung measures			
Lung intercedence	Location where lung crossed beneath sternum	Right lung	Left lung
	Below xiphisternal junction	$n = 3$	$n = 0$
	At xiphisternal junction	$n = 11$	$n = 0$
	Rib 1	$n = 0$	$n = 0$
	Rib 2	$n = 0$	$n = 4$
	Rib 3	$n = 3$	$n = 12$
	Rib 4	$n = 3$	$n = 16$
	Rib 5	$n = 9$	$n = 6$
	Rib 6/7	$n = 14$	$n = 3$
	Did not cross beneath sternum	$n = 2$	$n = 4$
	Lungs overlapped	$n = 17$ (37.8%)	
Liver measures			
Liver	40.6 ± 16.2 (10–81) mm		
Fat thickness measures			
Epicardial fat thickness	3.8 ± 2.1 (0–8) mm		
Apical fat thickness	4.0 ± 2.8 (0–16) mm		

Bony, cardiac, vascular, lung, liver, and fat measurements are reported for all patients ($n = 45$).
AP, anteroposterior; LV, left ventricular.
[a]LV mass is reported for $n = 38$ due to imaging contrast insufficiency in $n = 7$.

Table 4   **Anatomical factors and shock outcome**

Variable	Odds ratio estimate (95% CI)	*P*-value
BMI	0.772 (0.549–1.086)	0.138
Chest circumference (cm)	0.905 (0.783–1.045)	0.174
Rib cage AP (mm)	0.960 (0.903–1.021)	0.198
Rib cage left–right (mm)	**0.935 (0.877–0.997)**	**0.041**
Heart volume (cm^3)	0.998 (0.994–1.001)	0.220
Myocardium extent left	0.967 (0.871–1.074)	0.534
Myocardium extent posterior	**0.878 (0.781–0.986)**	**0.028**
LV myocardium thickness	1.006 (0.684–1.479)	0.977
LV mass	0.995 (0.979–1.011)	0.551
Apical fat (mm)	0.890 (0.661–1.198)	0.442
Inferior extent boundary of heart	**0.929 (0.865–0.998)**	**0.044**
Superior extent boundary of heart	**1.112 (1.011–1.222)**	**0.029**
Inferior-to-superior ratio	**0.287 (0.086–0.953)**	**0.042**
Sternum-to-heart distance	0.851 (0.687–1.053)	0.138
Maximum epicardial fat thickness	0.672 (0.387–1.164)	0.156

Reported are results of a univariate logistic regression model analysing anatomical parameter impact on shock failure for *n* = 41 patients. Anatomical factors with *P*-value < 0.05 are in bold.
BMI, body mass index; LV, left ventricular.

hearts that extended >40 mm above the xiphisternal junction, 31 of 32 subjects were defibrillation successes, while only 6 of 9 subjects with values <40 mm were successes. Expressed as a ratio, three of four subjects with defibrillation failure had an inferior-to-superior ratio >2, and only 3 of 41 subjects with a defibrillation success had a ratio this large.

Adverse events

Of the 45 subjects who underwent the substernal implantation procedure, there were no intra-procedural adverse events observed within the chronic pilot study and there were two intra-procedural adverse events in one subject within the acute ASD2 study, including one episode of transient atrial fibrillation during VF induction and reaction to anaesthesia resulting in low oxygen saturation. Both were resolved at the same day without sequelae.

Since ASD2 was an acute evaluation, adverse events observed in longer-term follow-up were only available for the chronic pilot study, with three-month results reported previously.[6]

Additional observations

Though not associated with an adverse event, the lead in one subject from the pilot study was observed by chest X-ray to be implanted in the left pleural cavity 1-day post-procedure. The lead and associated electrical performance have remained stable across follow-ups without subject discomfort; no interventions have been taken or are expected.

Discussion

Procedural safety

Implantation in the substernal space allows for lead positioning over the cardiac silhouette without entry into the pericardium, heart, or vasculature. The substernal space is routinely accessed for cardiac and non-cardiac procedures, and intra-operative complication, morbidity, and mortality rates associated with subxiphoid entry and/or substernal access are low; further, the sternocostal triangle point of entry near the xiphoid process is typically safe, reproducible, and absent vascular elements in humans.[7–11]

Limited analyses of the substernal space and surrounding anatomy have been presented previously. Kaneriya *et al.*[13] examined the average maximum width of the body of the human sternum (non-inclusive of manubrium), measuring 3.9 ± 0.9 cm in males (*n* = 27) and 3.5 ± 0.7 cm in females (*n* = 23), and reflecting our own findings (4.0 ± 0.8 cm). Similarly, Glassberg *et al.*[12] examined 100 consecutive CT scans of the human thorax to assess the relationship between the internal thoracic vessels and the sternal margin, and found that the mean distance from the sternal edge to the left internal thoracic vein measured 0.98 ± 0.23 cm, while the more distant left ITA measured 1.47 ± 0.30 cm. Glassberg's findings reflect our own, where the minimum separation between left sternal border and ITA was 1.3 ± 0.04 cm. In our study, no injury occurred to the ITA or its extension the superior epigastric artery, and there were no adverse events associated with small vessel bleeding related to the implant procedure. As such, the sternal body itself may provide a guide to facilitate safe substernal tunnelling and lead introduction without interaction with the internal thoracic vessels, and efforts undertaken to mark the midline and the left lateral border of the sternum prior to procedure may have contributed to low intra-procedural adverse events.

Because of the limited vascularity of the anterior mediastinum, small vessel bleeding-related adverse events were not observed, but given the relatively avascular nature of the substernal space, infection risk and treatment will need to be studied in a larger patient cohort. However, the substernal implant procedure does not disrupt the sternal bone, so the risk of serious sternal wound infection and
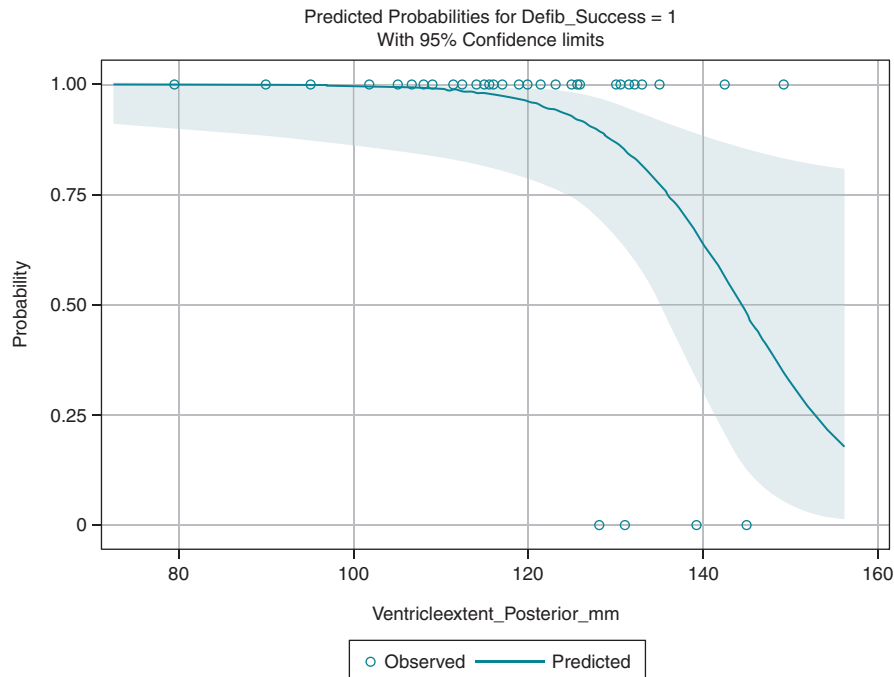
Figure 5 Defibrillation probability with increasing posterior myocardial extent. Defibrillation successes are recorded as open circles at 1.00 probability; defibrillation failures are recorded as open circles at 0.00 probability. Shading conveys the 95% confidence interval.

mediastinitis, such as is observed with sternotomy procedures, would be expected to be low with substernal lead implantation.[7]

The volume of the heart and the dimensions of the rib cage exhibited a large degree of variability across subjects, and the relationship of the two in terms of sternum-to-heart distance showed an overall range from 0 to 35 mm from the minimum to the maximum distance measured across subjects. During the substernal tunnelling procedure, the blunt tunnelling tool is directed upwards towards the sternum, and alternating AP and lateral fluoroscopic views are utilized to confirm the tunnelling trajectory. Despite no measurable sternum-to-heart separation in one subject, no instances of pericardial effusion were observed in this cohort. As reported previously,[6] there was one instance of mediastinal fibrosis encountered during the substernal tunnelling procedure, resulting in the implant procedure being abandoned before final system placement; this observation occurred in the subject with no sternum–heart separation measureable on CT. Thus, while imaging can provide information about sternum–heart distance, it may not reveal fibrosis. Mediastinal fibrosis has not been observed in any other subject across >120 cumulative subjects from feasibility studies conducted to date.[3–6]

While the lungs may cross beneath the sternum and, in a minority of patients, touch one another, the incision proximate the left aspect of the xiphoid process is devoid of lung. In our evaluation, the left lung did not cross beneath the sternum at or inferior to the xiphisternal junction in any subject. While in one subject the lead was observed to be implanted in the left pleural cavity 1-day post-procedure, there was no report of pneumothorax in this subject or >120 subjects from across human feasibility studies reported to date,[3–6] suggesting the lung may be resilient to penetration from a blunt tunnelling tool.

The relationship between hepatomegaly and congestive heart failure is known in medical literature.[16] There were no adverse events involving the liver, despite 87% of subjects having at least Class I heart failure.

Thus, despite a large range in values associated with anatomical parameters of potential importance to procedural safety, only two adverse events were encountered intra-procedurally, neither of which were associated with the tunnelling tool and both of which resolved the same day without sequelae; the only instance where tunnelling was abandoned intra-procedurally due to patient anatomy was in the subject with mediastinal fibrosis.

Aside from the pre-specified inclusion and exclusion criteria of each study included in this retrospective analysis,[5–6] pre-procedural imaging was not utilized to exclude patients based on specific anatomical parameters, unless the implanting physician determined that subject anatomy would not accommodate the implant tools. Among 113 total patients enrolled in the ASD2 and pilot studies, 3 patients (2.7%) did not proceed to implant based on medical judgement. The sternal tunnelling tool is malleable in nature with the intention of accommodating a wide variety of body habitus; thus, greater experience with substernal anatomy and implantation may allow for consideration of increasingly challenging anatomies or more limited exclusion criteria in the future.

Defibrillation efficacy

In our evaluation, defibrillation efficacy was 90% using a ≥ 10 J safety margin for testing, comparable with testing at implant with safety margin for TV ICD (88.8–92.1% in the SIMPLE study)[17] and SQ ICD (93.5% from the UNTOUCHED study).[18]

The QRS duration, inter-ventricular septum thickness, left ventricular mass, and mass index have been demonstrated as univariate predictors of defibrillation threshold for TV ICDs.[19] Differences in predictive findings suggest that underlying patient disease etiology may play a role in defibrillation efficacy. Predictors of SQ ICD defibrillation success have focused on parameters related to implant position optimization; fat beneath the coil or generator and anterior device placement are known to impact SQ ICD defibrillation performance negatively.[20]

In our analysis, 15 anatomical factors were evaluated for potential impact on defibrillation outcome. The left–right rib cage dimension, posterior reach of the heart, and low heart position measures showed *P*-values <0.05 in univariate analysis, with no significance found if adjusting for multiple comparisons.

Implant-related characteristics such as those of importance to SQ ICD[20] were not studied directly in our analysis. However, sternum-to-heart separation may provide a surrogate for subcoil fat, since the EV ICD lead tract is created close to the sternum and the mediastinum is composed predominantly of loose connective and adipose tissues. Sternum-to-heart distance was associated with a *P*-value of 0.1381 in univariate analysis. Future study with greater patient numbers and measurements of the separation between final defibrillation coil placement and the heart may provide a more accurate picture of subcoil fat importance. The QRS duration was not recorded for individual subjects in the ASD2 and pilot studies but may represent an important parameter for characterization in future analyses.

Finally, while studies such as PRAETORIAN[20] have relied on defibrillation predictors obtained from radiologic screening, most parameters used in our analysis, apart from BMI and chest circumference, were measured from CT images. However, radiographic imaging might be sufficient for measures such as rib cage dimensions or qualitative assessment of overall heart size or position. Similarly, transthoracic echocardiography might be useful in locating liver position or in manual measurements of the left-most and inferior-most heart extent. Intra-cardiac echocardiography might be relevant in measuring sternum-to-epicardium distance or apical fat. Because standard and non-standard echocardiography or radiographic measurements may be useful in simplifying clinical workflows without reliance on CT imaging, future evaluations would benefit from inclusion of these measures.

While only defibrillation performance was assessed for relationship to anatomical parameters in this study, patient anatomy may also have bearing on measures such as pacing threshold and R-wave amplitude. First-in-human chronic evaluation of pacing and sensing performance suggests that pacing capture is achieved in the vast majority of patients and that, while R-waves are smaller with the EV ICD than those observed with transvenous systems, there were no observations of inappropriate therapy as a result of oversensing in stably positioned substernal leads.[6,21]

A substernal alternative

The substernal space represents a compelling option for extravascular lead placement, potentially overcoming limitations of TV and SQ ICDs and providing the option for pacing therapies in a single extravascular device.[1,2,6] Because the substernal space offers a unique relationship between the defibrillation coil and surrounding anatomy, an understanding of anatomical and implantation factors will be required to maximize safety and efficacy for EV ICD.

Limitations

This work is intended to provide early signals of factors important to defibrillation efficacy and procedural safety for the EV ICD system but is limited by relatively small sample size from three countries based on retrospective analysis. The two studies evaluated had unique study designs and different inclusion and exclusion criteria, limiting comparability. Further, the ASD2 study included in this analysis predominantly used a cutaneous patch electrode *in lieu* of an implanted ICD, whereas the chronic pilot study utilized a fully implanted system to characterize defibrillation performance. In neither study was the patch or ICD location strictly specified. Future study will be needed to assess the impact of ICD location on defibrillation outcome. A limited number of anatomical parameters was evaluated for relation to defibrillation performance. Future study in a larger cohort, incorporating a wide range of anatomical parameters and potentially utilizing inputs from radiographic and echocardiography measures will be useful in more fully characterizing patient and implant variables of importance to procedure safety and defibrillation efficacy.

Conclusions

Quantified retrospective analysis of data from substernal feasibility evaluations and corresponding CT imaging showed two intra-procedural complications and 90% defibrillation success despite wide variation in patient anatomy. Collectively, the data suggest the ability to implant and defibrillate successfully across highly varied patient anatomies, but evaluation with a larger data set is needed to confirm these findings.

Data availability

Data were collected in two clinical trials; registrations are provided. All data presented were reviewed by a statistician. If needed, the data can be made available to the journal.

References

1. Bardy GH, Smith WM, Hood MA, Crozier IG, Melton IC, Jordaens L et al. An entirely subcutaneous implantable cardioverter-defibrillator. N Engl J Med 2010; **363**:36–44.
2. Theuns DA, Crozier IG, Barr CS, Hood MA, Cappato R, Knops R et al. Longevity of the subcutaneous implantable defibrillator: long-term follow-up of the European Regulatory Trial Cohort. Circ Arrhythm Electrophysiol 2015;**8**: 1159–63.
3. Chan JYS, Lelakowski J, Murgatroyd FD, Boersma LV, Cao J, Nikolski V et al. Novel extravascular defibrillation configuration with a coil in the substernal space: the ASD clinical study. JACC Clin Electrophysiol 2017;**3**:905–10.
4. Sholevar DP, Tung S, Kuriachan V, Leong-Sit P, Roukoz H, Engel G et al.; SPACE Study Investigators. Feasibility of extravascular pacing with a novel substernal electrode configuration: the Substernal Pacing Acute Clinical Evaluation study. Heart Rhythm 2018;**15**:536–42.
5. Boersma LVA, Merkely B, Neuzil P, Crozier IG, Akula DN, Timmers L et al. Therapy from a novel substernal lead: the ASD2 study. JACC Clin Electrophysiol 2019;**5**:186–96.
6. Crozier I, Haqqani H, Kotschet E, Shaw D, Prabhu A, Roubos N et al. First-in-human chronic implant experience of the substernal extravascular implantable cardioverter defibrillator. JACC Clin Electrophysiol 2020;**6**:1525–36.
7. Choi J, Yang H, Han J, Choi S. Manubrium-sparing median sternotomy as a uniform approach for cardiac operations. Tex Heart Inst J 2000;**27**:32–6.
8. Fonkalsrud E. Open repair of pectus excavatum with minimal cartilage resection. Ann Surg 2004;**240**:231–5.
9. Cakar F, Werner P, Augustin F, Schmid T, Wolf-Magele A, Sieb M et al. A comparison of outcomes after robotic open extended thymectomy for myasthenia gravis. Eur J Cardiothorac Surg 2007;**31**:501–4.
10. Baudoin Y-P, Hoch M, Protin X-M, Otton B-J, Ginon B, Voiglio E-J. The superior epigastric artery does not pass through Larrey's space (trigonum sternocostale). Surg Radiol Anat 2003;**25**:259–62.
11. Wei B, Bryant A, Minnich D, Cerfolio R. The safety and efficacy of mediastinoscopy when performed by general thoracic surgeons. Ann Thorac Surg 2014;**97**: 1878–84.
12. Glassberg R, Sussman S, Glickstein M. CT anatomy of the internal mammary vessels: importance in planning percutaneous transthoracic procedures. AJR Am J Roentgenol 1990;**155**:397–400.
13. Kaneriya D, Suthar K, Patel V, Umarvanshi B, Mehta C, Tailor C. Morphometric study of sternum for determination of sex. Cibtech J Bio Protoc 2013;**2**:6–13.
14. World Medical Association Declaration of Helsinki: ethical principles for medical research involving human subjects. JAMA 2013;**310**:2191–4.
15. Priori SG, Blomstrom-Lundqvist C, Mazzanti A, Blom N, Borggrefe M, Camm J. 2015 ESC guidelines for the management of patients with ventricular arrhythmias and the prevention of sudden cardiac death: the task force for the management of patients with ventricular arrhythmias and the prevention of sudden cardiac death of the European Society of Cardiology (ESC). Europace 2015;**17**:1601–87.
16. Maleki M, Vakilian F, Amin A. Liver diseases in heart failure. Heart Asia 2011;**3**: 143–9.
17. Neuzner J, Hohnloser SH, Kutyifa V, Glikson M, Dietze T, Mabo P et al. Effectiveness of single- vs. dual-coil implantable defibrillator leads: observations analysis from the SIMPLE study. J Cardiovasc Electrophysiol 2019;**30**:1078–85.
18. Boersma LV, El-Chami MF, Bongiorni MG, Burke M, Knops R, Aasbo J et al. Understanding outcomes with the S-ICD in primary prevention patients with low EF Study (UNTOUCHED): clinical characteristics and perioperative results. Heart Rhythm 2019;**16**:1636–44.
19. Hodgson D, Olsovsky M, Shorofsky S, Daly B, Gold M. Clinical predictors of defibrillation thresholds with an active pectoral pulse generator lead system. PACE 2002;**25**:408–13.
20. Quast A, Baalman S, Brouwer T, Smeding L, Wilde A, Burke M et al. A novel tool to evaluate the implant position and predict defibrillation success of the subcutaneous implantable cardioverter-defibrillator: the PRAETORIAN score. Heart Rhythm 2019;**16**:403–10.
21. Swerdlow CD, Zhang X, Sawchuk R, Greenhut S, Grinberg Y, Liu Y et al. Design and preliminary results of sensing and detection for an extravascular implantable cardioverter-defibrillator. JACC Clin Electrophys 2021;**7**:1387–99.